Southward Eddy Heat Transport Occurring along Southern Flanks of the Kuroshio Extension and the Gulf Stream in a 1/10° Global Ocean General Circulation Model

KUNIHIRO AOKI

Faculty of Environmental Earth Science, Hokkaido University, Sapporo, Japan

SHOSHIRO MINOBE

Department of Natural History Sciences, Graduate School of Science, Hokkaido University, Sapporo, Japan

YOUICHI TANIMOTO

Faculty of Environmental Earth Science, Hokkaido University, Sapporo, and Research Institute for Global Change, Japan Agency for Marine-Earth Science and Technology, Yokohama, Japan

YOSHIKAZU SASAI

Research Institute for Global Change, Japan Agency for Marine-Earth Science and Technology, Yokohama, Japan

(Manuscript received 9 November 2012, in final form 10 May 2013)

ABSTRACT

The present study investigates meridional heat transport induced by oceanic mesoscale variability in the World Ocean using a 1/10° global ocean general circulation model (OGCM) running on the Earth Simulator. The results indicate prominent poleward eddy heat transport around the western boundary currents and the Antarctic Circumpolar Current, and equatorward eddy heat transport in the equatorial region, consistent with the previous studies using coarse-resolution OGCMs. Such poleward eddy heat transport in midlatitude oceans suggests that the eddies act to reduce meridional background temperature gradients across the currents, as would be expected based on baroclinic instability. Interestingly, however, along the southern flanks of the eastward jets of the Kuroshio Extension and the Gulf Stream, southward eddy heat transport occurs in subsurface layers. This is likely due to the southward migration of warm water cores originating from southern areas adjacent to these currents. Southward movement of these cores is caused by interactions with unsteady meanders and cold eddies detaching from the meanders. The potential impact on biological production in the subtropical surface layers of these southward-traveling warm water cores is also discussed.

1. Introduction

Mesoscale variability, which has spatial scales from tens to hundreds of kilometers and temporal scales from tens to hundreds of days, occurs as mesoscale eddies, Rossby waves, and current meanders. The energy and transport associated with mesoscale variability are often referred to as ''eddy energy'' and ''eddy transport,'' respectively. Mesoscale phenomena are quite vigorous, as the kinetic energy associated with eddies exceeds the mean kinetic energy over most of the ocean (Wyrtki et al. 1976; Richardson 1983). Also, eddy transport plays an important role in transporting heat (e.g., Jayne and Marotzke 2002), freshwater (e.g., Meijers et al. 2007), and even nutrients (e.g., Sumata et al. 2010).

A number of attempts have been made to estimate meridional eddy heat transport, whose contribution to the total meridional heat transport in the ocean cannot be ignored (e.g., Jayne and Marotzke 2002). Analyses of hydrographic (Berstein and White 1982; Bennett and White 1986) and mooring (Wunsch 1999) data suggested that meridional eddy heat transport is large around the western boundary currents (WBCs), though these in situ data cannot reveal the spatial structure of global eddy

Corresponding author address: Kunihiro Aoki, Graduate School of Environmental Earth Science, Hokkaido University, N10W5, Sapporo 060-0810, Japan.
E-mail: aokik@ees.hokudai.ac.jp

DOI: 10.1175/JPO-D-12-0223.1

heat transport. Investigations of eddy heat transport using satellite data have advantages over in situ observations in terms of spatial coverage and resolution. However, because information obtained by satellites is limited to the sea surface, the eddy heat fluxes below the surface must be assumed. For example, the eddy heat transport has been estimated by analogy with mixing length theory (Holloway 1986; Keffer and Holloway 1988; Stammer 1998) or using an assumption of effective depth of the eddy heat fluxes (Qiu and Chen 2005).

Given the limitations of observational estimations of eddy heat transport, ocean general circulation models (OGCMs) have been used instead. Jayne and Marotzke (2002) showed that meridional eddy heat transport in mid- and high-latitude regions is strong in the neighborhood of the WBCs and the Antarctic Circumpolar Current (ACC). The OGCMs used in previous studies were, however, either coarse-resolution global models (Jayne and Marotzke 2002; Meijers et al. 2007; Volkov et al. 2008) or higher-resolution models such as a $^1/_{10}°$ model for the Atlantic (Smith et al. 2000) or a $^1/_{12}°$ model for the North Pacific (Yim et al. 2010). No global estimation of eddy heat transport has yet been conducted using a high-resolution OGCM, and thus it is difficult to compare the characteristics and mechanisms of eddy heat transport across basins. In the present study, we investigate meridional eddy heat transport using a quasi-global high-resolution OGCM for the first time and examine the similarities and differences in its characteristics in different regions.

The remainder of the present paper is organized as follows. Section 2 outlines the configuration of the OGCM used in the present study, together with the methodology for computing eddy heat transport. In section 3, the horizontal and vertical structure of eddy heat transport is described, and the interesting phenomenon of southward eddy heat transport along the southern flanks of the Kuroshio Extension and the Gulf Stream is highlighted. The underlying cause of this phenomenon is also explored. In section 4, a summary and discussion are presented.

2. Data and methods

We analyze output of the simulation by OGCM for the Earth Simulator (OFES; Masumoto et al. 2004), which is a quasi-global OGCM conducted by the Earth Simulator Center (ESC). The model domain extends from 75°S to 75°N with a horizontal resolution of $^1/_{10}°$ and has 54 depth levels. The OFES simulation was performed using surface momentum flux derived from Quick Scatterometer (QuikSCAT) satellite data (Kubota et al. 2002) taken in August 1999 (Sasaki et al. 2006). Details of the model configuration are described in Masumoto et al. (2004). In this study, three-day snapshots from 1 January 2003 to 31 December 2007 (5 years) provided by ESC were analyzed.

The time-mean horizontal eddy heat transport vector in 5 years is calculated by $\rho c_p \langle \mathbf{v}' T' \rangle$, where ρ is the density of seawater, c_p is the heat capacity of seawater at a constant pressure, and $\mathbf{v}'$ and T' denote the eddy components of horizontal velocity and temperature, respectively. The angle brackets indicate a 5-yr mean. Each eddy component is defined as an anomaly from the 3-month mean, based on the fact that the time scale of mesoscale variability is generally less than 100 days (e.g., Fu and Cazenave 2001), where each 3-month mean is defined as the average performed in each nonoverlapping 3-month interval: average in 1 January–31 March, 1 April–30 June, and so on. Thus, the averaging operator shown in the angle brackets can be written as $\langle \cdot \rangle = \tau^{-1}(\int_{\Omega_1} dt + \int_{\Omega_2} dt + \cdots + \int_{\Omega_N} dt) = \tau^{-1} \sum_{i=1}^{i=N} \int_{\Omega_i} dt$, where $\Omega_i (i = 1, 2, \ldots, N)$ represents the aforementioned temporal intervals, and τ is the temporal interval for 5 years. Subscript N should take 20 in this case because 5 years are divided into 20 temporal intervals. The zonal scale of eddies based on this definition is about 2.5°–5.0° in OFES (not shown), which is similar to the scale reported from satellite observations (Chelton et al. 2007).

In the 5-yr average, the total heat transport equals the sum of the heat transport by the 3-month-mean field and the eddy heat transport: $\rho c_p \langle \mathbf{v} T \rangle = \rho c_p \langle \overline{\mathbf{v}}^3 \overline{T}^3 \rangle + \rho c_p \langle \mathbf{v}' T' \rangle$, where variables with a superscript of 3 with overbar represent the 3-month-mean components. The heat transport by the 3-month-mean field is referred to in this study as large-scale heat transport. One may consider that $\rho c_p \langle \mathbf{v} T \rangle = \rho c_p \langle \overline{\mathbf{v}}^3 \overline{T}^3 \rangle + \rho c_p \langle \mathbf{v}' T' \rangle + \rho c_p \langle \overline{\mathbf{v}}^3 T' \rangle + \rho c_p \langle \mathbf{v}' \overline{T}^3 \rangle$. However, the covariance terms between the eddy component and the large-scale component equal zero, that is, $\langle \overline{\mathbf{v}}^3 T' \rangle = \langle \mathbf{v}' \overline{T}^3 \rangle = 0$, because the integrals of $\overline{\mathbf{v}}^3 T'$ and $\mathbf{v}' \overline{T}^3$ for each 3-month interval are zero, respectively.

3. Results

a. Horizontal and vertical distributions of eddy heat transport

As a beginning, we will examine where large eddy heat transport occurs. The results of the present study indicate prominent poleward eddy heat transport around the WBCs and the ACC and equatorward eddy heat transport in the equatorial region (Figs. 1 and 2). The horizontal and meridional distributions of meridional eddy heat transport are qualitatively similar to those estimated using coarser-resolution OGCMs (Jayne and

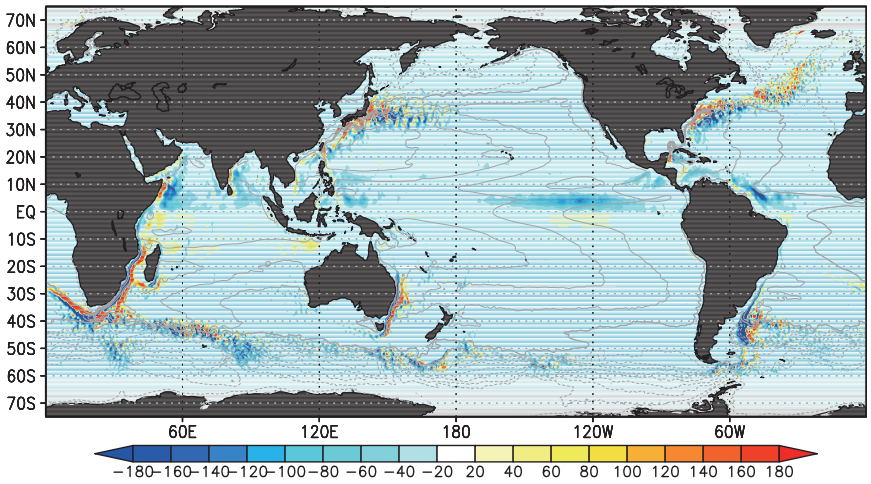

FIG. 1. Global distribution of vertically integrated meridional eddy heat transport (10^6 W m^{-1}). Positive (negative) values indicate northward (southward) heat transport. Contours denote the 5-yr-mean sea surface height with a contour interval (CI) of 20 cm.

Marotzke 2002; Meijers et al. 2007; Volkov et al. 2008). The large poleward eddy heat transport around the WBCs and the ACC suggests that the eddies act to weaken strong meridional background temperature gradients, as would be expected from baroclinic instability. In the northern midlatitudes, large northward eddy heat transports occur at the latitude of the Kuroshio Extension in the North Pacific (about 37.0°N) and at the latitude of the Gulf Stream in the North Atlantic (about 37.0°N). Although the magnitudes of these eddy heat transports are similar, their relative contribution to the total meridional heat transport is larger for the North Pacific than for the North Atlantic. This is because large-scale meridional heat transport associated with the Atlantic meridional overturning circulation is significant. In the southern midlatitudes, large southward eddy heat transport exceeding total heat transport occurs at latitudes of 50.0°–40.0°S. Most of the eddy heat transport in this latitude band is associated with the Agulhas Return Current and the Brazil–Malvinas Current.

An interesting phenomenon found in the present study is southward eddy heat transport around latitudes to the south of the Kuroshio Extension and the Gulf Stream (Fig. 2). Although similar southward eddy heat transport was predicted by Yim et al. (2010) using a high-resolution North Pacific model (Fig. 2 in their paper), they did not examine the cause of this phenomenon. The southward eddy heat transport has a maximum of 0.09 PW at around 34.0°N in the North Pacific and of 0.06 PW at around 33.5°N in the North Atlantic, just to the south of the current axes of the Kuroshio Extension and the Gulf Stream, respectively. They cannot be ignored because these magnitudes correspond to 50%–70% of the northward eddy heat transport occurring around the latitudes of the Kuroshio Extension (0.13 PW at 37°N) and the Gulf Stream (0.11 PW at 37°N), respectively. The southward eddy heat transport is predominant at subsurface levels, in contrast to the northward eddy heat transport, which occurs at the near surface (Fig. 3). The depth at which the maximum southward eddy heat transport occurs is 600 m in the North Atlantic, which is larger than the corresponding depth of 400 m in the North Pacific.

To examine the horizontal structure of the southward eddy heat transport, the divergent component of the vertically integrated eddy heat transport is calculated. Because the method for computing the divergent component in this study is exactly the same as that in Jayne and Marotzke (2002), we explain it here briefly. The vertically integrated eddy heat transport can be defined as Helmholtz decomposition:

$$\mathbf{F} \equiv [\langle \mathbf{v}' T' \rangle] = \mathbf{k} \times \nabla\psi + \nabla\phi, \tag{1}$$

where square brackets denote vertical integration, $\mathbf{k}$ is a vertical unit vector, ψ and ϕ are like a streamfunction and a velocity potential, respectively. The first and the second terms on the rhs in (1) give rotational and divergent components, respectively. Generally, although one can introduce other decompositions (e.g., Eden et al. 2007), this decomposition enables us to obtain the divergent component whose zonal integration equals the zonally integrated meridional eddy heat transport shown in Fig. 2. Taking divergence of (1), we obtain a Poisson equation for the potential of the divergent component:

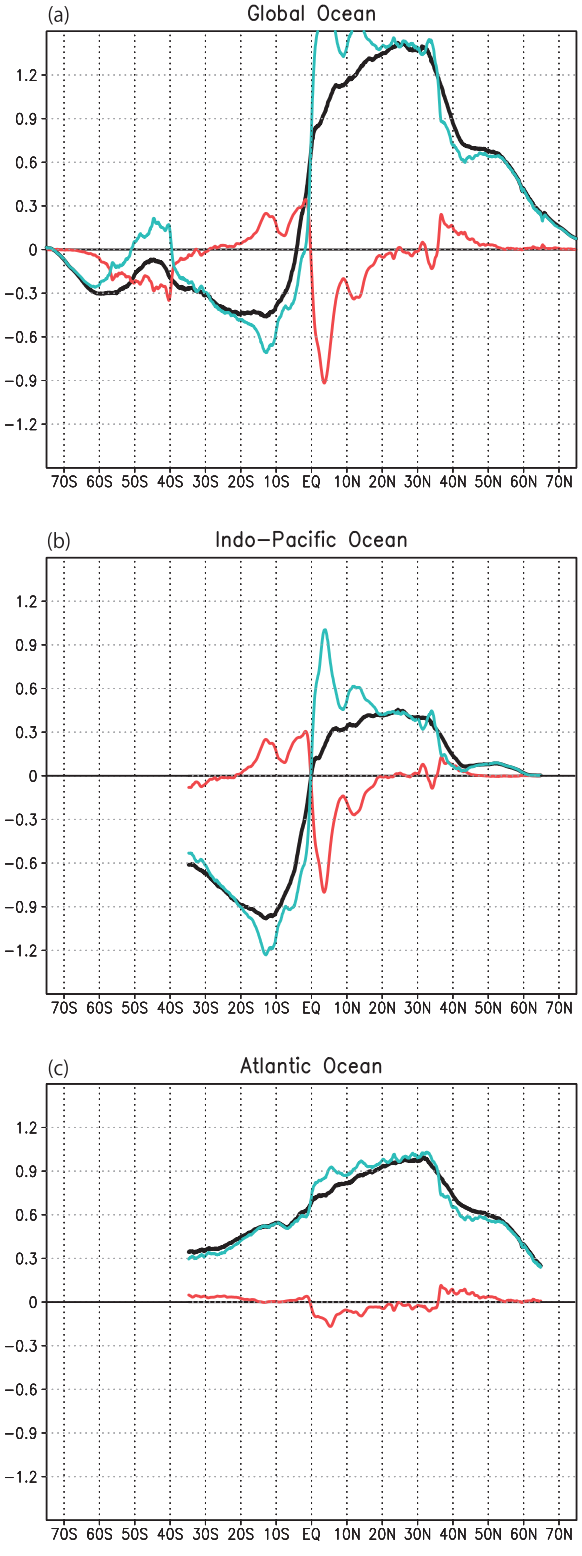

FIG. 2. Meridional distribution for (a) the global ocean, (b) the Indo-Pacific Ocean, and (c) the Atlantic Ocean of zonally and vertically integrated meridional total (black), large-scale (blue), and eddy (red) heat transport (PW).

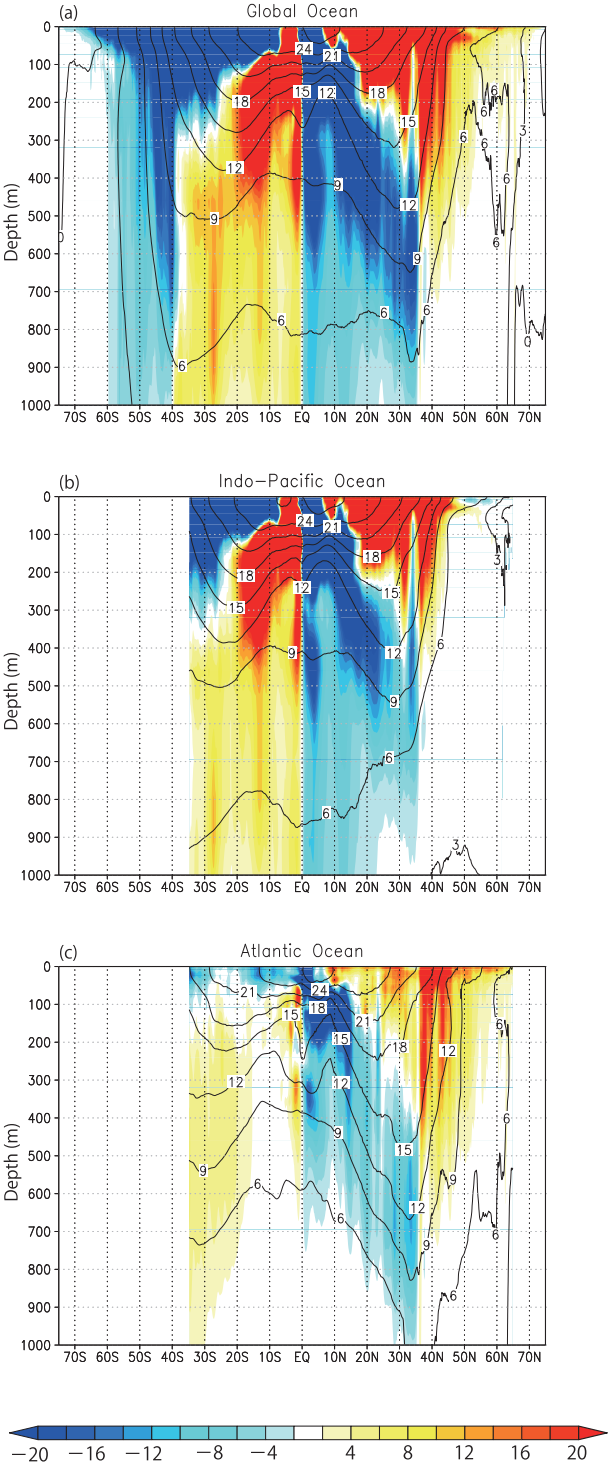

FIG. 3. Meridional-vertical view of zonally integrated meridional eddy heat transport for (a) the global ocean, (b) the Indo-Pacific Ocean, and (c) the Atlantic Ocean (10^{10} W m^{-1}). Contours represent zonally averaged 5-yr-mean temperature (°C).

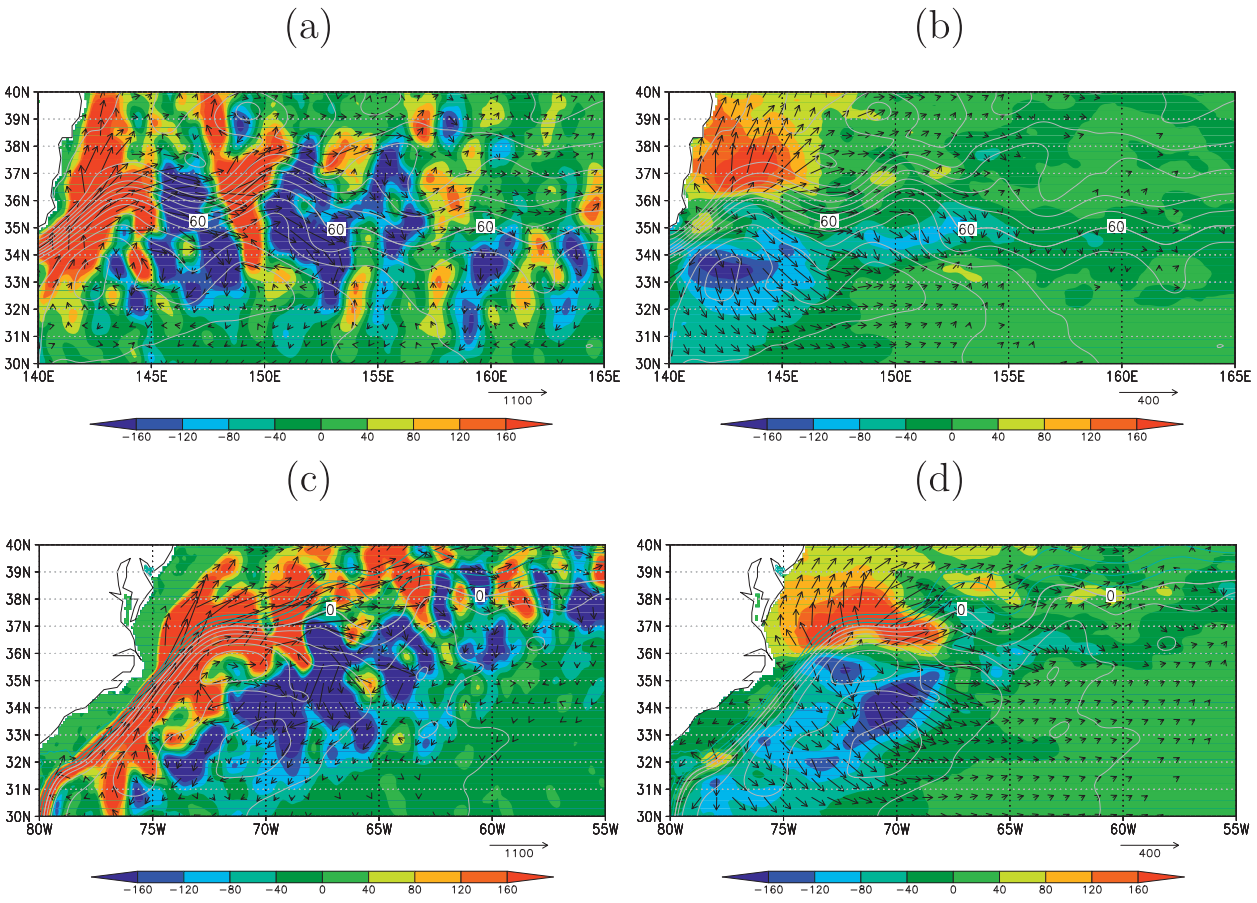

FIG. 4. Eddy heat transport vector for (a),(c) original vertically integrated eddy heat transport and (b),(d) its divergent component for the (top) Kuroshio Extension and (bottom) Gulf Stream (10^6 W m^{-1}). The background color shading is the meridional component of the eddy heat transport. The contours represent 5-yr-mean sea surface height.

$$\nabla^2\phi = \nabla \cdot \mathbf{F}. \tag{2}$$

We can solve this equation with appropriate lateral boundary conditions. In OFES there is no horizontal velocity through the lateral boundaries between the ocean and the lands. Thus, it is reasonable to set no eddy heat transport through the boundaries. From (1), this gives the following boundary condition for (2),

$$\nabla\phi \cdot \mathbf{n} = 0, \tag{3}$$

where $\mathbf{n}$ is a unit vector perpendicular to the lateral boundaries. Although it is mathematically valid to choose the boundary condition with the sum of the rotational and divergent components, this choice may bring an unphysical result because it allows us to consider that each component depends on each other, implying inconsistency to the definition (1).

Fig. 4 shows the original vertically integrated eddy heat transport and its divergent component. The original meridional eddy heat transport has a wavelike structure, with positive and negative values alternatively occurring in the zonal direction, and this structure is caused by rotational eddy heat transport, as noted in previous studies (Jayne and Marotzke 2002; Qiu and Chen 2005). In contrast, the divergent eddy heat transport exhibits a smooth distribution, with a generally northward (southward) trend in the region to the north (south) of the mean current axis of the Kuroshio Extension (the Gulf Stream). Unlike the eddy heat transport expected from baroclinic instability, most of the southward divergent eddy heat transport along the southern flank of these currents occurs in a direction opposite to that of the mean meridional temperature gradient at the depth of the maximum southward eddy heat transport (not shown). The position where the maximum southward eddy heat transport occurs is 33.0°N, 142.5°E for the Kuroshio Extension and 34.0°N, 70.5°W for the Gulf Stream. Note that these latitudes are slightly different from those for the maximum southward eddy heat

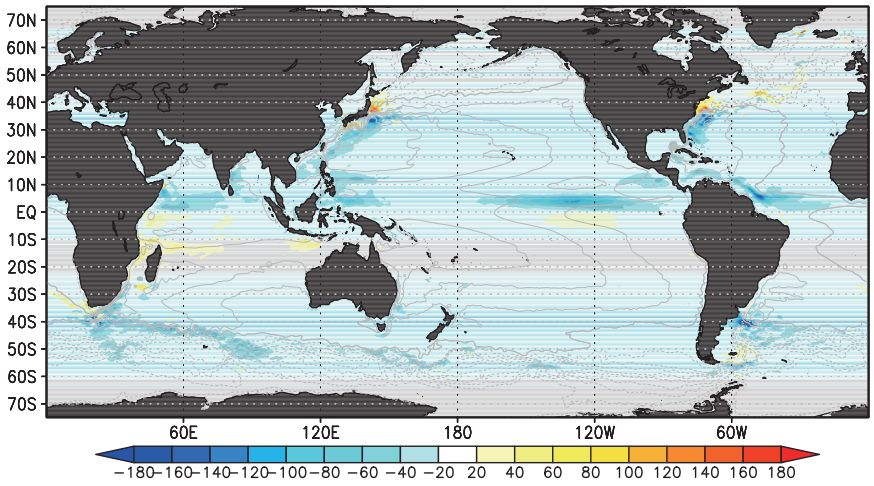

FIG. 5. As in Fig. 1, but for meridional divergent component of vertically integrated eddy heat transport.

transport obtained from the zonally integrated meridional eddy heat transport. This is because weak but broad northward divergent eddy heat transport occurs to the east of the region of the southward divergent eddy heat transport. Different from the Kuroshio Extension and the Gulf Stream, equatorward eddy heat transports around the Agulhas Return Current and the Brazil–Malvinas Current are not found (Fig. 5), although large southward eddy heat transports occur as mentioned above.

b. *Origin of southward eddy heat transport along southern flank of the Kuroshio Extension and the Gulf Stream*

In section 3a, it was seen that southward eddy heat transport commonly occurs both in the Kuroshio Extension and the Gulf Stream regions. It occurs at subsurface levels along the southern flanks of these eastward jets. The origin of this southward eddy heat transport is unlikely to be explained by baroclinic instability. This subsection therefore explores the cause for this phenomenon.

The meridional eddy heat transport in the divergent component shown in Fig. 4 is equivalent to the meridional exchange of warm and cold water. For example, a northward divergent eddy heat transport implies a northward transfer of warm water and/or a southward transfer of cold water. Likewise, a southward divergent eddy heat transport implies a southward transfer of warm water and/or a northward transfer of cold water. Thus, to examine meridional transfer of water around the region just to the south of the Kuroshio Extension and the Gulf Stream, subsurface temperature snapshots in these regions are examined.

Figure 6 shows a series of temperature snapshots for the Kuroshio Extension region at a depth of 400 m, that is, the depth at which the maximum southward eddy heat transport occurs. These snapshots indicate that a core of warm water is being advected by ambient flow of cold eddies in the Kuroshio Extension region. In the early stage of this process, an area of warm water extends south of the Kuroshio Extension, with a core around 34.0°N, 144.0°E (‘‘W’’ in Fig. 6a). This warm water has a source upstream of the WBC of the North Pacific. Simultaneously, the Kuroshio Extension has a small meander at 147.5°E (‘‘M1’’) and a large meander at 151.0°E (‘‘M2’’), both of which later grow and from which two cold eddies become detached. The warm water core begins to move southward when the southward flow on the western side of a detached cold eddy (‘‘C1’’) reaches the location of the warm water core (Fig. 6b). The core then moves counterclockwise along the periphery of the cold eddy, moving first southward and then northward (Figs. 6c,d). It again moves southward when it encounters a southward flow induced on the western side of a second cold eddy (‘‘C2’’) (Fig. 6e). Subsequently, the warm water core forms a vortex pair with a cold eddy to the south (‘‘C3’’) and moves westward (Fig. 6f).

Similar to the case for the Kuroshio Extension, southward movement of a warm water core is also seen in the Gulf Stream region at 600-m depth, where the maximum southward eddy heat transport occurs (Fig. 7). The core is initially formed off Cape Hatteras around 36.0°N, 69.0°W (‘‘W’’ in Fig. 7a) and exhibits a more circular shape than that for the Kuroshio Extension. Similar to the case for the Kuroshio Extension, the source of the warm water is upstream of the WBC of the North Pacific. Simultaneously, the Gulf Stream meanders toward the south at about 66.5°W (‘‘M’’).

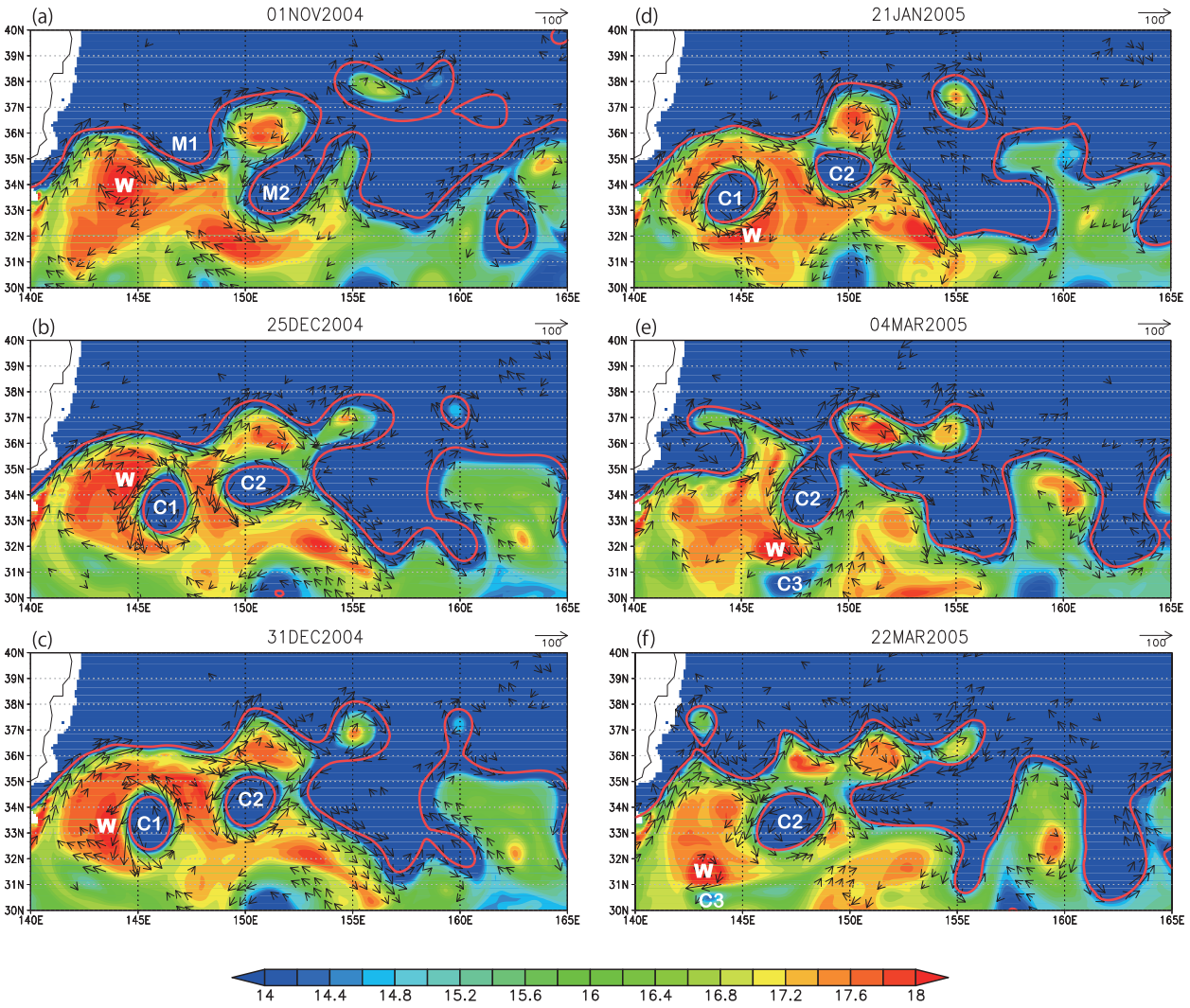

FIG. 6. (a)–(f) Snapshots of temperature field at 400-m depth (color shading) around the Kuroshio Extension during the period 1 Nov 2004–22 Mar 2005. Vectors denote horizontal velocities larger than 10 cm s^{-1}. Red contour denotes a sea surface height of 60 cm, which is a proxy for the Kuroshio Extension axis. Markers "M," "C," and "W" refer to meanders, cold eddies, and warm water cores, respectively. See the text for more details.

As the meander grows, southward flow of the meandering current advects the warm water core toward the south (Figs. 7b,c). The core is stretched along the east–west direction by the meridional shear near the trough of the large meander and is divided into two warm water cores (Figs. 7d,e). These cores are advected southward by southward flow of two cold eddies ("C1" and "C2"), which detach from the Gulf Stream meander (Fig. 7f), as in the case of the Kuroshio Extension.

The warm water cores penetrate to greater depths for the Gulf Stream than for the Kuroshio Extension. Figure 8 shows the vertical structure around these cores. The isotherms are downwardly concave, with the equivalent temperature surfaces being deeper for the Gulf Stream than for the Kuroshio Extension. In addition, the main thermocline, defined as the maximum vertical temperature gradient (color shading in Fig. 8), is deeper for the Gulf Stream (920 m) than the Kuroshio Extension (750 m) by 170 m. This difference in the penetration depth of warm water is likely to be related to the difference in the depth of the maximum southward eddy heat transport for the Gulf Stream and the Kuroshio Extension shown in Fig. 3.

To examine whether the occurrence of warm water cores is a general feature of the regions investigated, rather than being limited to a specific period, the frequency of occurrence of high-temperature water was investigated. First, to establish a definition of "high

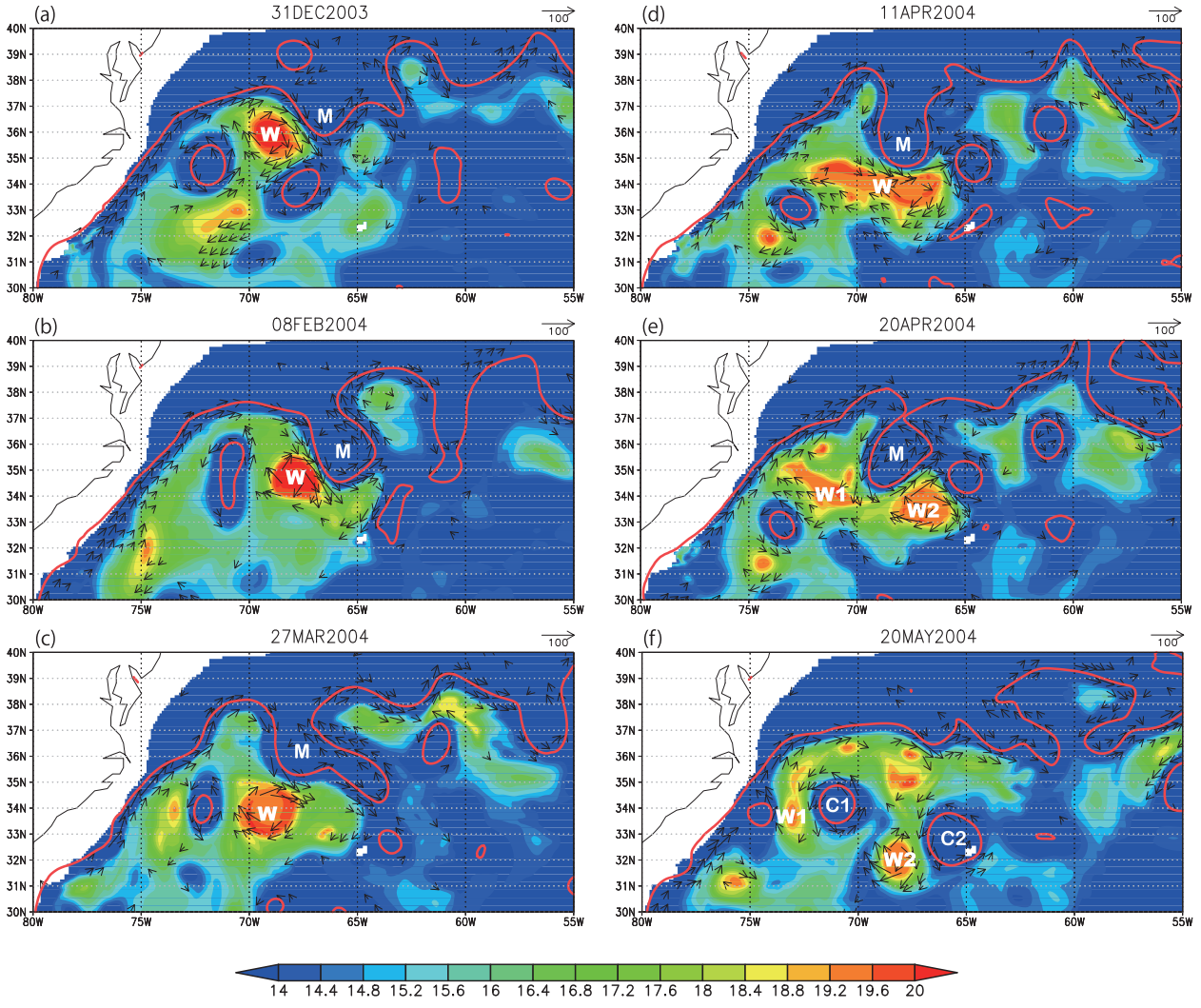

FIG. 7. (a)–(f) Snapshots of temperature field at 600-m depth (color shading) around the Gulf Stream during the period 31 Dec 2003–20 May 2004. Vectors denote horizontal velocities larger than 10 cm s^{-1}. Red contour denotes a sea surface height of 0 cm, which is a proxy for the Gulf Stream axis. Markers "M," "C," and "W" refer to meanders, cold eddies, and warm water cores, respectively. See the text for more details.

temperature," temperature histograms were examined for a depth of 400 m in the Kuroshio Extension region (30°–40°N and 140°–165°W) and 600 m in the Gulf Stream region (30°–40°N and 80°–55°W). The results indicated a frequency minimum at 18.0°C for the Kuroshio Extension region and 18.5°C for the Gulf Stream region (not shown). Consequently, high-temperature water was defined as water with a temperature above 18.0°C for the Kuroshio Extension and 18.5°C for the Gulf Stream.

The color shading in Fig. 9 indicates the occurrence frequency of temperatures above 18.0°C (18.5°C) at the depth of 400 m (600 m) for the Kuroshio Extension (the Gulf Stream). The results show that warm water frequently occurs in regions just south of the first ridge of the stationary meander of the Kuroshio Extension (34.0°N, 144.0°E), and just south of the Gulf Stream after it separates from the coast (35.0°N, 71.0°W) in this simulation (cf. contours in Fig. 4). We may, in passing, note that the locations of the first ridge of the meander and the separation point of these currents are similar to that shown in observation (Richardson et al. 1978; Mizuno and White 1983). Interestingly, these regions roughly correspond to the regions of southward divergent eddy heat transport (contours in Fig. 9). This suggests that the southward divergent eddy heat transport reflects southward advection of warm water cores from just south of the Kuroshio Extension and the Gulf Stream, as seen in the temperature snapshot data.

As discussed above, cold eddies and unsteady meanders are likely to influence the southward migration of

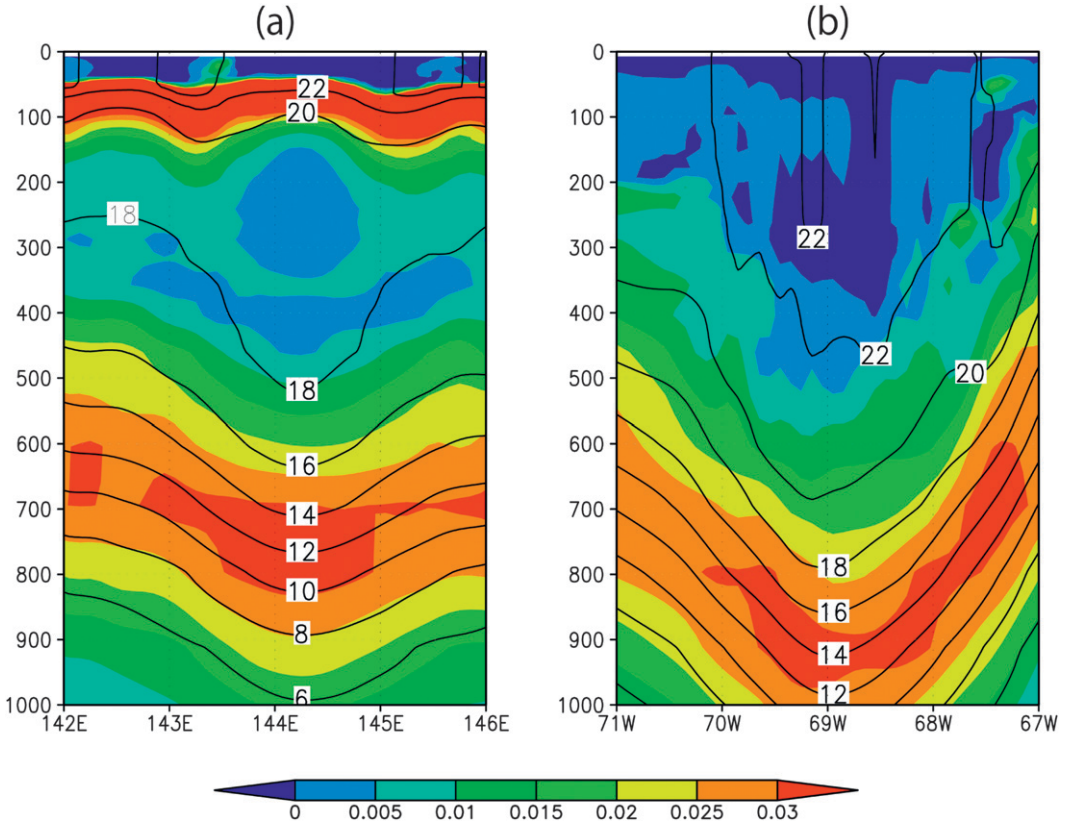

FIG. 8. Vertical temperature structure (°C; contours where CI is 2°C) and its vertical derivative (°C m^{-1}; color shading) within warm water cores occurring in early stage of snapshot data for the (a) Kuroshio Extension (Fig. 7a) and (b) Gulf Stream [in (a)].

warm water cores. This can be confirmed by examining the horizontal skewness distribution of subsurface temperature (Fig. 10). Skewness is a measure of the asymmetry of the probability distribution, and positive (negative) skewness indicates that a lobe of the probability distribution expands in the direction of positive (negative) values of the variable. It is found that negative skewness tends to occur in the area of southward divergent eddy heat transport. This reflects the intermittent occurrence of large negative temperature anomalies. Such anomalies are caused by the passage of well-developed cold eddies or large southward meanders. As seen in the snapshot data, these strong cold eddies became separated from the main current axes of the Kuroshio Extension and the Gulf Stream. The negative skewness appearing within the area of southward divergent eddy heat transport suggests that strong cold eddies influence the southward movement of warm water cores.

4. Summary and discussion

The present study investigated meridional eddy heat transport using OFES, a global OGCM with a 1/10° horizontal resolution. Similar to the results of previous studies using coarser-resolution OGCMs, the present study indicates prominent poleward eddy heat transport around the WBCs and the ACC and equatorward eddy heat transport in the equatorial region. However, large southward eddy heat transport occurs at subsurface levels along the southern flanks of the Kuroshio Extension and the Gulf Stream. Such a southward eddy heat transport does not occur in the global 1/4° OGCM by Jayne and Marotzke (2002). Major differences between this study and theirs are the definition of the eddy component and horizontal resolution. The former, however, cannot be the case because the southward eddy heat transport does occur even in the same definition as they adopted in which the eddy is defined as an anomaly from temporal mean over the period (not shown). Given that the North Pacific model with 1/12° resolution simulates southward eddy heat transport for the Kuroshio Extension by Yim et al. (2010; Fig. 2 in their paper), the occurrence of the southward eddy heat transport could be because of an increased resolution of the model.

The southward eddy heat transport for the Kuroshio extension and the Gulf Stream is associated with the

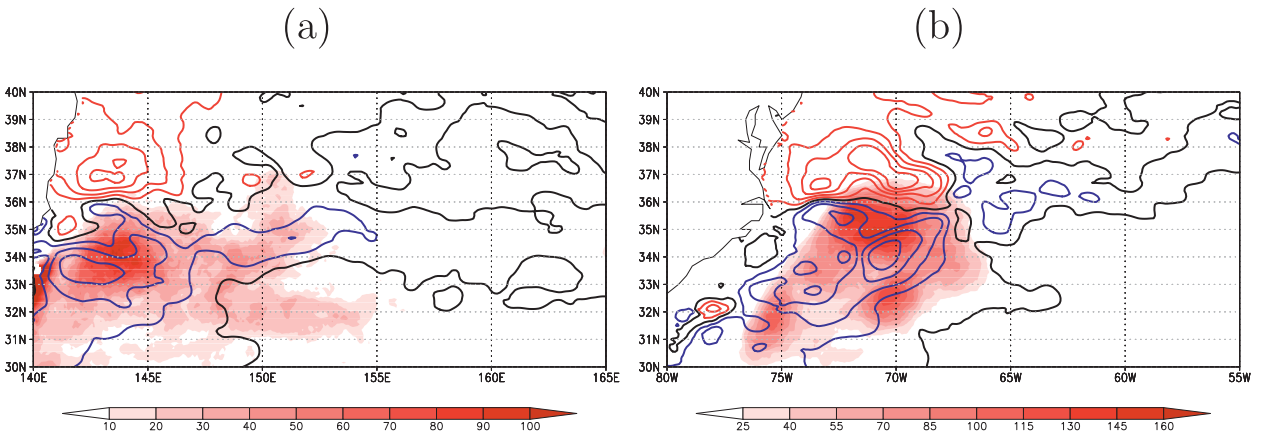

FIG. 9. Frequency of occurrence of temperatures warmer than (a) 18.0°C at depth of 400 m for Kuroshio Extension and (b) 18.5°C at depth of 600 m for Gulf Stream (color shading). Contours denote meridional component of divergent eddy heat transport with a CI of 50×10^6 W m^{-2}, where red (blue) contours correspond to northward (southward) eddy heat transport and black contours denote zero line of eddy heat transport.

southward migration of warm water cores originating from just south of the eastward jets of these currents. The southward migration of these cores is likely due to advection by ambient flow of cold eddies and unsteady southward meanders. These cold eddies are detached from well-grown meanders of the Kuroshio Extension or the Gulf Stream.

Such behavior of the warm and cold eddies suggests that the southward eddy heat transport is a secondary effect of baroclinic instability. According to the baroclinic instability theory, disturbance will grow in a background baroclinically unstable eastward jet and becomes well-developed warm and cold eddies to the north and south of the eastward jet, respectively, accompanied by northward eddy heat transport in the Northern Hemisphere (e.g., Pedlosky 1987). Such a phenomenon has also been confirmed in both observational studies (Richardson et al. 1978; Mizuno and White 1983) and the present study. However, the southward eddy heat transport occurs just south of the Kuroshio Extension and the Gulf Stream in this study, different from the expectation from baroclinic instability. To resolve this conflict, it is necessary to take into account the fact that in the Kuroshio Extension and the Gulf Stream warm water supplied from upstream is located along these currents. To the south of these currents, the cold eddies resulting from baroclinic instability can play a role in transporting the warm water toward the south. Thus, southward eddy heat transport occurs along the southern flanks of these currents. In the Agulhas Return Current and the Brazil–Malvinas Current, however, corresponding northward eddy heat transport does

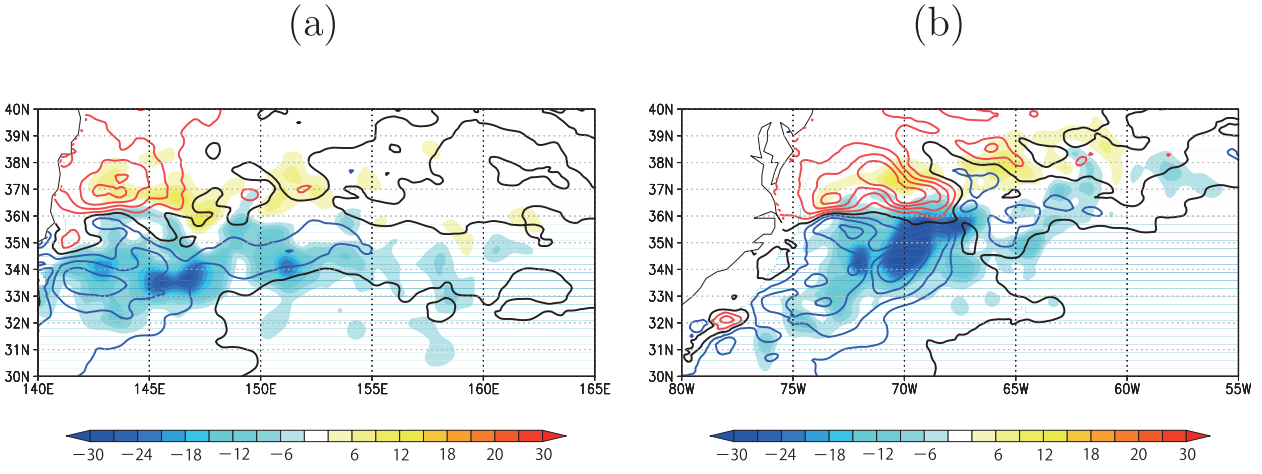

FIG. 10. Skewness of temperature (°C^3) at (a) depth of 400 m for Kuroshio Extension and (b) depth of 600 m for Gulf Stream. Contours denote meridional component of divergent eddy heat transport with a CI of 50×10^6 W m^{-2}, where red (blue) contours correspond to northward (southward) eddy heat transport, and black contour denotes zero line of eddy heat transport.

not occur along the northern flanks of these currents, although the warm water is located along the current. This suggests that the presence of the warm water along the eastward jet is necessary, but additional conditions may be required to cause the equatorward eddy heat transport.

Southward movement of warm water cores to the south of the Kuroshio Extension and the Gulf Stream may also be important for transport of tracers such as nutrients. Such nutrients are important for marine ecosystems; higher nutrient concentrations generally give rise to a higher primary production in the surface euphotic zone, particularly in oligotrophic subtropical regions (e.g., Oschlies and Garcon 1998). It is known that the largest amount of nutrient transport occurs along the Kuroshio Extension and the Gulf Stream, and this phenomena is referred to as ''the nutrient stream'' (Pelegri et al. 1996; K. Komatsu 2012, personal communication), suggesting that these currents play an important role in nutrient transport. The southward migration of warm water cores, whose sources are the WBCs, may be a mechanism by which nutrients can be transported toward oligotrophic subtropical regions. Nutrients within a warm water core can be released to the surface either by upwelling caused by the ascent of the seasonal thermocline (McGillicuddy et al. 2007) or vertical convection triggered by strong surface cooling in winter (Williams et al. 2000). Several warm water cores in the present study had a structure similar to the so-called mode water eddy, which is the anticyclonic eddy accompanied by a raised seasonal thermocline located near the surface and depressed main thermocline (McGillicuddy et al. 2007) (Fig. 8a), suggesting that the former mechanism for nutrient supply might play a role. On the other hand, other eddies were found to have thermostads extending from the surface to a depth of several hundred meters (Fig. 8b), suggesting that the latter mechanism may also be at work.

We have described the occurrence of the southward eddy heat transport for the Kuroshio Extension and the Gulf Stream and suggested a possible explanation for these phenomena. It is interesting that this study found the eddy heat transport unexplained by hitherto known baroclinic instability alone. However, this study also posed several questions. 1) Are the southward eddy heat transports in the Kuroshio Extension and the Gulf Stream general features in the simulations with high resolution? 2) Why does it appear only for the Kuroshio Extension and the Gulf Stream, when there is another strong eastward jet such as the Agulhas Return Current or the Brazil–Malvinas Current? Those issues are expected to be explored using higher-resolution OGCMs and simple theoretical models. Also, we have discussed biological impacts of the southward-traveling warm eddies. This can be clarified in further studies using physical–biological coupled models, in the future.

Acknowledgments. The present study was supported by Grants-in-Aid (21740336, 22106008, 22106006, 22340132, 22340135, and 22106007) for Scientific Research from the Ministry of Education, Science, Sports, and Culture and the funds from the research program Population Outbreak of Marine Life (POMAL) of the Ministry of Agriculture, Forestry, and Fisheries, both in Japan. The authors also thank the anonymous reviewers and the editor for helpful comments.

REFERENCES

Bennett, A., and W. White, 1986: Eddy heat flux in the subtropical North Pacific, 1. *J. Phys. Oceanogr.,* **16,** 728–740.

Berstein, R. L., and W. B. White, 1982: Meridional eddy heat Flux in the Kuroshio Extension Current. *J. Phys. Oceanogr.,* **12,** 154–159.

Chelton, D. B., M. G. Schlax, R. M. Samelson, and R. A. de Szoeke, 2007: Global observations of large oceanic eddies. *Geophys. Res. Lett.,* **34,** L15606, doi:10.1029/2007GL030812.

Eden, C., R. J. Greatbatch, and D. Olbers, 2007: Interpreting eddy fluxes. *J. Phys. Oceanogr.,* **37,** 1282–1296.

Fu, L. L., and A. Cazenave, 2001: *Satellite Altimetry and Earth Sciences: A Handbook of Techniques and Applications.* International Geophysics Series, Vol. 69, Academic Press, 463 pp.

Holloway, G., 1986: Estimation of oceanic eddy transports from satellite altimetry. *Nature,* **323,** 243–244.

Jayne, S. R., and J. Marotzke, 2002: The oceanic eddy heat transport. *J. Phys. Oceanogr.,* **32,** 3328–3345.

Keffer, T., and G. Holloway, 1988: Estimating southern ocean eddy flux of heat and salt from satellite altimetry. *Nature,* **332,** 624–626.

Kubota, M., N. Iwasaka, S. Kizu, M. Konda, and K. Kutsuwada, 2002: Japanese ocean flux data sets with use of remote sensing observations (J-OFURO). *J. Oceanogr.,* **58,** 213–225.

Masumoto, Y., and Coauthors, 2004: A fifty-year eddy-resolving simulation of the World Ocean: Preliminary outcomes of OFES (OGCM for the Earth Simulator). *J. Earth Simul.,* **1,** 35–56.

McGillicuddy, D. J., and Coauthors, 2007: Eddy/wind interactions stimulate extraordinary mid-ocean plankton blooms. *Science,* **316,** 1021–1026.

Meijers, A. J., N. L. Bindoff, and J. L. Roberts, 2007: On the total, mean, and eddy heat and freshwater transports in the Southern Hemisphere of a $^1/_8° \times {}^1/_8°$ global ocean model. *J. Phys. Oceanogr.,* **37,** 277–295.

Mizuno, K., and W. B. White, 1983: Annual and interannual variability in the Kuroshio Currents system. *J. Phys. Oceanogr.,* **13,** 1847–1867.

Oschlies, A., and V. Garcon, 1998: Eddy-induced enhancement of primary production in a model of the North Atlantic Ocean. *Nature,* **394,** 266–269.

Pedlosky, J., 1987: *Geophysical Fluid Dynamics.* Springer-Verlag, 710 pp.

Pelegri, J. L., G. T. Csanady, and A. Martins, 1996: The North Atlantic nutrient stream. *J. Oceanogr.,* **52,** 275–299.

Qiu, B., and S. Chen, 2005: Eddy-induced heat transport in the subtropical North Pacific from Argo, TMI, and altimetry measurements. *J. Phys. Oceanogr.,* **35,** 458–473.

Richardson, P. L., 1983: Eddy kinetic energy in the North Atlantic Ocean from surface drifters. *J. Geophys. Res.,* **88,** 4355–4367.

——, R. E. Cheney, and L. V. Worhington, 1978: A census of Gulf Stream rings, Spring 1975. *J. Geophys. Res.,* **83,** 6136–6144.

Sasaki, H., Y. Sasai, M. Nonaka, Y. Masumoto, and S. Kawahara, 2006: An eddy-resolving simulation of the quasi-global ocean driven by satellite-observed wind field. *J. Earth Simul.,* **6,** 35–49.

Smith, R. D., M. E. Maltrud, F. O. Bryan, and M. W. Hecht, 2000: Numerical simulation of the North Atlantic Ocean at 1/10°. *J. Phys. Oceanogr.,* **30,** 1532–1561.

Stammer, D., 1998: On eddy characteristics, eddy transports, and mean flow properties. *J. Phys. Oceanogr.,* **28,** 727–739.

Sumata, H., and Coauthors, 2010: Effect of eddy transport on the nutrient supply into the euphotic zone simulated in an eddy-permitting ocean ecosystem model. *J. Mar. Syst.,* **83,** 67–87.

Volkov, D. L., T. Lee, and L. L. Fu, 2008: Eddy-induced meridional heat transport in the ocean. *Geophys. Res. Lett.,* **35,** L20601, doi:10.1029/2008GL035490.

Williams, R. G., A. J. McLaren, and M. J. Follows, 2000: Estimating the convective supply of nitrate and implied variability in export production over the North Atlantic. *Global Biogeochem. Cycles,* **14,** 1299–1313.

Wunsch, C., 1999: Where do ocean eddy heat fluxes matter? *J. Geophys. Res.,* **104** (C6), 13 235–13 249.

Wyrtki, K., L. Magaard, and J. Hager, 1976: Eddy energy in the oceans. *J. Geophys. Res.,* **81,** 2641–2646.

Yim, B. Y., Y. Noh, B. Qiu, S. H. You, and J. H. Yoon, 2010: The vertical structure of eddy heat transport simulated by an eddy-resolving OGCM. *J. Phys. Oceanogr.,* **40,** 340–353.